JOC The Journal of Organic Chemistry

Featured Article

pubs.acs.org/joc

Laterally π-Extended Dithia[6]helicenes with Heptagons: Saddle-Helix Hybrid Molecules

Takao Fujikawa,[†] Yasutomo Segawa,*[,†,‡] and Kenichiro Itami*[,†,‡,§]

[†]Graduate School of Science and [§]Institute of Transformative Bio-Molecules (WPI-ITbM), Nagoya University, Chikusa, Nagoya 464-8602, Japan

[‡]JST, ERATO, Itami Molecular Nanocarbon Project, Chikusa, Nagoya 464-8602, Japan

Supporting Information

ABSTRACT: A laterally π-extended dithia[6]helicene **1**, representing an interesting saddle-helix hybrid molecule containing an unusual heptagon, has been synthesized by $MoCl_5$-mediated oxidative stitching of tetrakis(thienylphenyl)naphthalene precursor **2** involving reactive-site capping by chlorination and subsequent Pd-mediated dechlorination of tetrachlorinated intermediate **1-Cl$_4$**. Highly distorted, wide helical structures of dithia[6]helicenes (**1** and **1-Cl$_4$**) were clarified by single-crystal X-ray diffraction analyses where heterochiral slipped π–π stacking was displayed in a one-dimensional fashion. Notably, theoretical studies on the thermodynamic behavior of **1** predicted an extraordinarily high isomerization barrier of 49.7 kcal·mol^{-1}, which enabled optical resolution and chiroptical measurements. Electronic structures of these huge helicenes were also examined by photophysical and electrochemical measurements.

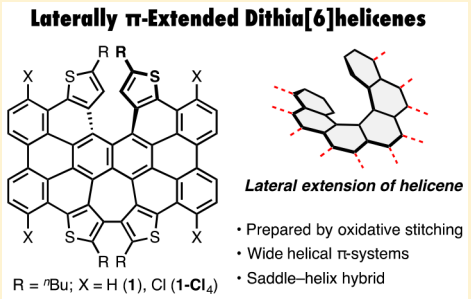

INTRODUCTION

Helicenes are helical, *ortho*-fused polyaromatic compounds whose π-electron systems are characterized by nonplanarity, chiroptical properties, and unique dynamic behavior.[1] To exploit the peculiar properties of helicenes in materials science, a variety of chemical modifications about the helix have been attempted despite the innate difficulty of constructing such highly crowded structures. In particular, the π-extension of the helical motif (Figure 1a) results in a significant perturbation of the optoelectronic properties and control over solid-state aggregation as well as molecular dynamics.[2] In this context, the helical elongation approach has been historically studied in the synthesis of carbo- and hetera[*n*]helicenes (*n* is the number of fused rings), as exemplified by the recent synthesis of triple-layered carbo[16]helicenes and long oxahelicenes (Figure 1b).[3] The lateral π-extension approach has also become frequent in recent years.[4−6] Compared with the simplicity of the former approach, the latter has a significant flexibility in molecular design. Synthetic work related to benzo- and pyrenohelicenes has dominated the field,[4,5] and recently, corannulene- and perylene-based helicenes have also appeared, in which the characters of fused polyaromatic moieties such as dynamic motion and redox ability were merged with helical properties.[6a−c] In these laterally π-extended helicenes, however, the helix is partially fused with polyaromatic moieties. A fully fused congener has never been reported except in theoretical studies due to synthetic difficulties with accessing this structure.[7] As groundwork toward the preparation of these helical nanoarchitectures, we report herein the rapid synthesis of dithia[6]helicenes **1** and **1-Cl$_4$**, saddle-helix hybrid molecules featuring wide laterally extended helical π-systems (Figure 1c).

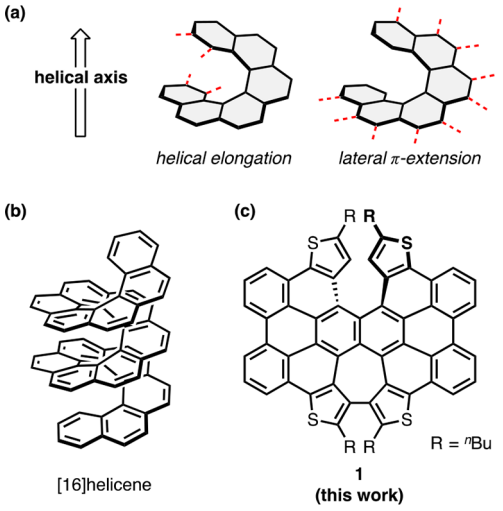

Figure 1. (a) Two π-extension approaches in helicene chemistry. The chemical structures of (b) [16]helicene as an example of helical elongation and (c) laterally π-extended dithia[6]helicene **1** synthesized in this work.

RESULTS AND DISCUSSION

Synthesis. Recently, we reported the synthesis of double helicene **3-Cl$_4$** from tetrakis(thienylphenyl)naphthalene precursor **2** by the oxidative cyclodehydrogenation followed by the

Received: June 21, 2017
Published: July 7, 2017

DOI: 10.1021/acs.joc.7b01540
J. Org. Chem. 2017, 82, 7745−7749

in situ chlorination in the presence of 20 equiv of $MoCl_5$ under a nitrogen atmosphere (Scheme 1).[8] To our surprise, treating

Scheme 1. Synthesis of Double Helicenes 3-Cl_4 and 3 (Previous Work) and Laterally Extended Helicenes 1-Cl_4 and 1 (This Work)

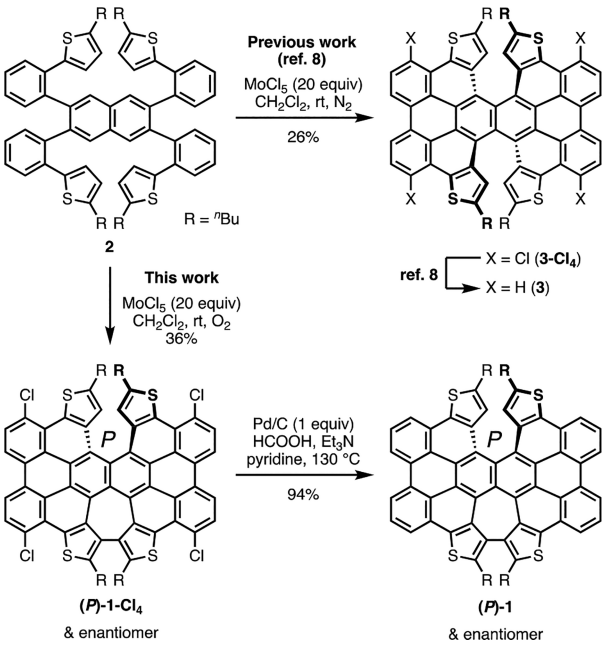

an oxygen-saturated dichloromethane as solvent effectively pushed one additional C−C bond formation at the dithia[6]-helicene moiety of **3-Cl_4**, resulting a saddle-helix hybrid molecule **1-Cl_4**.[9] It is of note that the formation of a heptagonal ring (a dithiahexa[7]circulene framework) occurred under mild conditions.[10,11] As with the same conditions in the synthesis of **3**, Pd-mediated dechlorination[8] can be accomplished yielding **1**. The compounds **1-Cl_4** and **1** are poorly soluble in non-halogenated organic solvents but show somewhat better solubility in halogenated ones.

Structural Analyses. The assumed structures of dithia[6]-helicenes **1-Cl_4** and **1** were confirmed by ^1H and ^{13}C NMR spectra and mass spectroscopy. For example, a moderate shielding effect, one of the characteristics of helicene, appeared as the upfield shift of the singlet peaks in the ^1H NMR spectra corresponding to the hydrogen atoms at the end of the inner helix (δ 6.39 and 6.35 ppm for **1-Cl_4** and **1**, respectively). To add firm support, single-crystal X-ray diffraction analyses were carried out using racemic crystals of **1-Cl_4** and **1**. The former were obtained from recrystallization of **1-Cl_4** from chloroform as cocrystals with chloroform molecules, while the latter were obtained from recrystallization of **1** from hot nitrobenzene. As depicted in Figure 2, refined X-ray structures corroborated our assumed structures, exhibiting global distortion of π-surfaces.

The π-skeletons of **1-Cl_4** and **1** consist of three structural components: a helical dithia[6]helicene motif, a saddle-shaped dithiahexa[7]circulene motif, and relatively planar bilateral motifs. Helical distortions of dithia[6]helicene motifs were evaluated by the distances between the two carbon atoms at the helical termini (C19−C32 = 3.462(7) Å for **1-Cl_4**; C2−C2′ = 3.308(5) Å for **1**) and the splay angles (C20−C24−C26−C31 = 58.3(4)° for **1-Cl_4**; C3−C24−C24′−C3′ = 56.6(3)° for **1**). Both values in the X-ray structures were reproduced in the

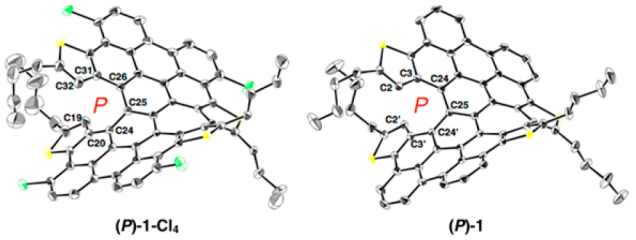

Figure 2. ORTEP drawings of (*P*)-isomers of **1-Cl_4** and **1** with thermal ellipsoids shown at 50% probability (the hydrogen atoms, the minor part of the disordered moieties, and solvent molecules are omitted for clarity).

optimized structures of **TetraMe-1-Cl_4** and **TetraMe-1**, methyl analogues of **1-Cl_4** and **1**, calculated at the B3LYP/6-31G(d) level of theory (3.45 Å and 60.6° for **TetraMe-1-Cl_4**; 3.40 Å and 57.7° for **TetraMe-1**). Meanwhile, a significant disparity in these values is recognized when compared with those in the optimized structure of 2,13-dimethyldithia[6]helicene **4** (3.07 Å and 46.4°), presumably attributed to the stretching force along the helical axis derived from the negatively curved heptagonal ring of the adjoining dithiahexa[7]circulene motif. Simultaneously, the heptagonal ring annulation compresses the helix in a direction vertical to the helical axis as probed by the reduced inner C−C−C bond angles (Figure S2). For example, the central bond angles inside the helices of **1-Cl_4** and **1** are markedly smaller than that of **4** by almost 5° (C24−C25−C26 = 119.9(4)° for **1-Cl_4**; C24−C25−C24′ = 120.7(3)° for **1**; C(14b)−C(14c)−C(14d) = 125.75° for **4**). The sum of five inner bond angles also results in smaller values for **1-Cl_4** (619.5°) and **1** (624.5°) than for **4** (634.9°), which indicates an enlarged eclipse of the helical termini. The relatively planar bilateral motifs of both dithia[6]helicenes are key points of heterochiral slipped one-dimensional $\pi-\pi$ stacking arrays (Figure S4). Whereas the interplanar distance ($d_{\pi-\pi}$) of 3.48 Å indicates moderate $\pi-\pi$ interactions through the one-dimensional column of **1-Cl_4**, a broader $d_{\pi-\pi}$ of 3.69 Å in the crystal of **1** indicates weak $\pi-\pi$ interactions. Large cofacial overlap was realized in both cases, which is one of the important merits of lateral π-extension.[8,12]

Theoretical Studies on Configurations. Next, the enantiomeric interconversion pathway of **TetraMe-1** was examined theoretically (B3LYP/6-31G(d)). In addition to the helicity of the dithia[6]helicene motif, steric repulsion between the two *n*-butyl groups in the bay region of the dithiahexa[7]-circulene motif manifests as another helicity. Accordingly, besides the most stable isomers ((*P*,*P*)- and (*M*,*M*)-**TetraMe-1**, ΔG = 0.0 kcal·mol^{-1}) observed in the X-ray crystallography, metastable diastereomers ((*P*,*M*)- and (*M*,*P*)-**TetraMe-1**, ΔG = 14.7 kcal·mol^{-1}) exist, where the two different helical motifs possess opposite helicity (helicity notation in the left top of Figure 3). In the enantiomerizations, two distinct transition states were found: one involves the inversion of the dithiahexa[7]circulene motif via a planarization of the heptagonal ring (TS1, ΔG = 29.1 kcal·mol^{-1}) and the other involves the inversion of the dithia[6]helicene motif via a face-to-face orientation of the terminal aromatic rings (TS2, ΔG = 49.7 kcal·mol^{-1}). The isomerization barrier estimated for **TetraMe-1** (49.7 kcal·mol^{-1}) is an extraordinarily high value compared with that for **4** (39.3 kcal·mol^{-1} at the same calculation level),[13] which is probably due to the heptagonal ring distortion and the steric congestion of the alkyl groups at

DOI: 10.1021/acs.joc.7b01540
J. Org. Chem. 2017, 82, 7745−7749

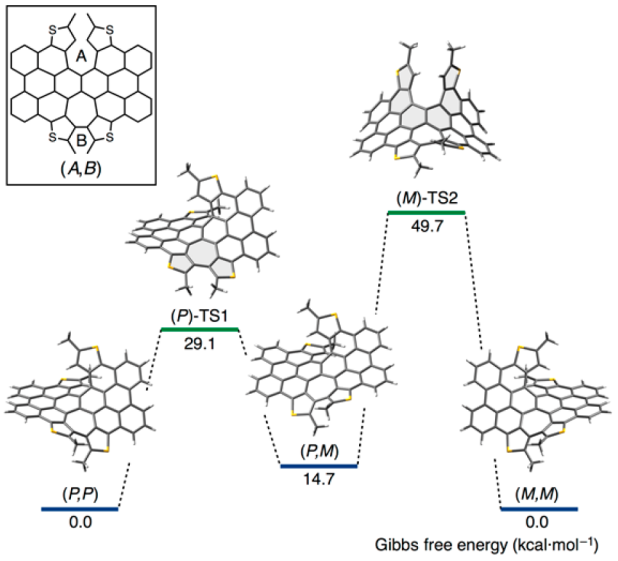

Figure 3. Enantiomeric interconversion pathways of **TetraMe-1** (enantiomeric structures of (*M*)-TS1, (*P*)-TS2, and (*M*,*P*)-**TetraMe-1** and the pathways among them are omitted for clarity). Relative Gibbs free energies (ΔG) were calculated at the B3LYP/6-31G(d) level of theory at 298.15 K and 1 atm. The *n*-butyl groups were replaced with methyl groups to simplify the calculations.

the bay region during the transition. The barriers for enantiomerization of **TetraMe-1** are large even when compared with related barriers for double-layered carbo[*n*]helicene (41.7−43.5 kcal·mol^{-1} as experimental values with n = 7−9).[14]

Optical Resolution and Optical Properties. The high isomerization barrier of **1** enabled its optical resolution by means of HPLC equipped with a COSMOSIL chlorester column (Figure S1). The specific rotation of the fast-moving enantiomer was determined to be $[\alpha]^{22}_{D}$ −1439 (c = 0.00018), and its circular dichloism (CD) spectrum exhibited negative Cotton effects at 501 nm ($\Delta\varepsilon$ = −82 M^{-1}·cm^{-1}) and 471 nm ($\Delta\varepsilon$ = −44 M^{-1}·cm^{-1}) and positive Cotton effects at 421 nm ($\Delta\varepsilon$ = +111 M^{-1}·cm^{-1}), 398 nm ($\Delta\varepsilon$ = +75 M^{-1}·cm^{-1}), and 326 nm ($\Delta\varepsilon$ = +54 M^{-1}·cm^{-1}) (Figure 4a). By comparing with the simulated CD spectrum, the fast-moving enantiomer was assigned as (−)-(*P*,*P*)-**1**. The slow-moving isomer gave a mirror-image CD spectrum, which was assigned as (+)-(*M*,*M*)-**1**.

The UV−vis absorption spectra of **1-Cl$_4$** and **1** exhibit two major absorption bands, i.e., longer wavelength absorption with clear vibronic structures and intense absorption around 400 nm (Figure 4b). Absorption maxima for **1-Cl$_4$** are observed at 518 nm (ε = 2.7 × 10^4 M^{-1}·cm^{-1}), 486 nm (ε = 2.2 × 10^4 M^{-1}·cm^{-1}), 455 nm (ε = 1.6 × 10^4 M^{-1}·cm^{-1}), and 404 nm (ε = 8.0 × 10^4 M^{-1}·cm^{-1}). In comparison, these maxima are blue-shifted for **1** appearing at 502 nm (ε = 2.1 × 10^4 M^{-1}·cm^{-1}), 472 nm (ε = 1.8 × 10^4 M^{-1}·cm^{-1}), 442 nm (ε = 1.2 × 10^4 M^{-1}·cm^{-1}), and 394 nm (ε = 7.0 × 10^4 M^{-1}·cm^{-1}). TD-DFT calculations (B3LYP/6-31G(d)) attributed the longer wavelength absorption bands to HOMO → LUMO transition (S_1, f_{calc} = 0.1889 for **TetraMe-1-Cl$_4$** and 0.1690 for **TetraMe-1**) and the intense absorption bands to almost equal contribution of HOMO−2 → LUMO and HOMO → LUMO+2 transitions (S_6, f_{calc} = 0.7023 for **TetraMe-1-Cl$_4$** and 0.7626 for **TetraMe-1**). The fluorescence spectra also show a similar tendency in the spectral shift with that in absorption, giving maxima at 530 and 566 nm for **1-Cl$_4$** (Φ_F = 0.37), and at 514 and 548 nm for **1** (Φ_F = 0.23). These photophysical spectra of **1-Cl$_4$** and **1** were similar to those of the corresponding double helicene analogues **3-Cl$_4$** and **3** but slightly blue-shifted in both cases.

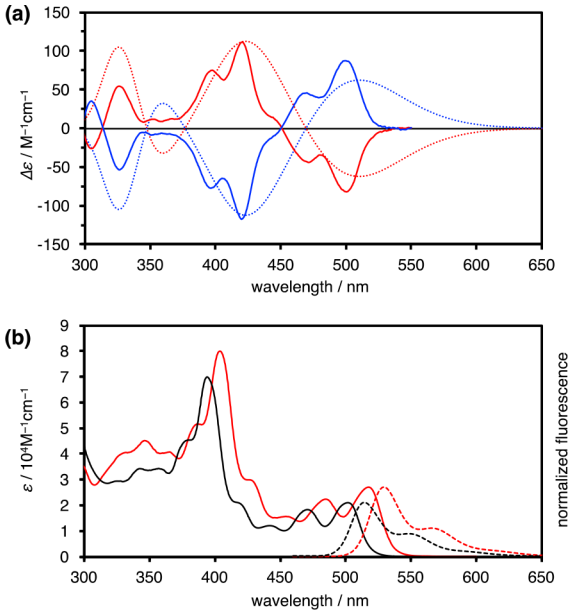

Figure 4. (a) Experimental circular dichroism spectra of the fast-moving enantiomer ((−)-**1**, red solid line) and the slow-moving enantiomer ((+)-**1**, blue solid line) in HPLC and simulated circular dichroism spectra of (*P*,*P*)-**TetraMe-1** (red dotted line) and (*M*,*M*)-**TetraMe-1** (blue dotted line) calculated at the B3LYP/6-31G(d) level of theory. (b) UV−vis absorption (solid lines) and fluorescence (dotted lines) spectra of **1-Cl$_4$** (red) and **1** (black). Chloroform solutions were used for all photophysical measurements.

Electrochemical Studies. Frontier molecular orbitals were computationally estimated to be lower for **TetraMe-1-Cl$_4$** than for **TetraMe-1** due to the presence of electron-accepting chloride groups (E_{HOMO} = −5.07 eV and E_{LUMO} = −2.34 eV for **TetraMe-1-Cl$_4$**; E_{HOMO} = −4.85 eV and E_{LUMO} = −2.05 eV for **TetraMe-1**), which apparently perturb electronic states as observed in the photophysical properties. To elucidate the electrochemical behavior of these structures, cyclic voltammetry was performed in dichloromethane solutions containing 0.1 M of TBAPF$_6$ (vs Fc/Fc$^+$). The voltammograms exhibited two-step oxidation waves, whose first steps were reversible ($E_{1/2}$ = 0.50 V for **1-Cl$_4$**, 0.43 V for **1**) and second steps were irreversible (E_p = 0.84 V for **1-Cl$_4$**, 0.83 V for **1**) at scan rate of 0.1 V·s^{-1} (Figure 5). Because the double helicenes **3-Cl$_4$** and **3** exhibited reversible two-step oxidation waves under the same conditions, the existence of saddle-shaped structural motifs derived from the heptagonal rings apparently destabilized the oxidized species after the second oxidation events. The slight anodic shift of the first oxidation potential (0.07 V) upon chlorination reflects the differences in the estimated HOMO energies. Hence, the chloride groups provide an opportunity not only for further synthetic diversification (at the resulting C−Cl bonds) but also for important electronic modifications.

■ CONCLUSION

In summary, laterally π-extended dithia[6]helicenes containing an unusual heptagonal ring have been synthesized, isolated, purified, and fully characterized. A chlorinated dithia[6]helicene **1-Cl$_4$** was obtained by treating tetrakis(thienylphenyl)-naphthalene precursor **2** with a large excess of MoCl$_5$ under

DOI: 10.1021/acs.joc.7b01540
J. Org. Chem. 2017, 82, 7745−7749

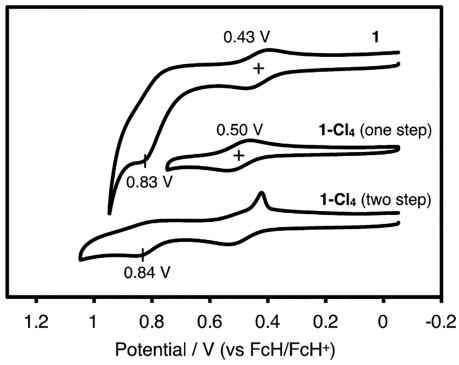

Figure 5. Cyclic voltammograms of **1-Cl$_4$** and **1** in dichloromethane containing 0.1 M of $TBAPF_6$ at scan rate of 0.1 V·s^{-1}. FcH = ferrocene.

oxygen atmosphere, and subsequent Pd-mediated reduction afforded fully dechlorinated dithia[6]helicene **1**. Highly distorted, wide helical structures of dithia[6]helicenes (**1** and **1-Cl$_4$**) were unambiguously determined by single-crystal X-ray diffraction analyses. One-dimensionally stacked molecular arrays were presented utilizing the large π-surfaces of relatively planar bilateral motifs. An extraordinarily high isomerization barrier (49.7 kcal·mol^{-1}) was predicted theoretically for **1**, suggesting its excellent chiral stability. Indeed, optical resolution of **1** was achieved by the chiral HPLC, which enabled chiroptical measurements. Electronic states of **1-Cl$_4$** and **1** were also examined by photophysical, electrochemical, and theoretical studies, and the effects of chloride atom substitution and heptagonal ring formation were revealed. Although fully fused wide helicenes have attracted researchers' interests because of their physicochemical properties, a lack of synthetic methodology has hampered development in this area. A rapid synthetic approach reported herein will not only accelerate the chemistry of laterally π-extended helicenes but also stimulate molecular design for unprecedented helical nanoarchitectures.

EXPERIMENTAL SECTION

General Methods. Unless otherwise noted, all materials including dry solvents were obtained from commercial suppliers and used without further purification. Compound **2** was prepared according to the procedure reported in the literature.[13] Unless otherwise noted, all reactions were performed with dry solvents under an atmosphere of nitrogen in dried glassware with standard vacuum-line techniques. All workup and purification procedures were carried out with reagent-grade solvents in air.

Analytical thin-layer chromatography (TLC) was performed using E. Merck silica gel 60 F_{254} precoated plates (0.25 mm). The developed chromatogram was analyzed by UV lamp (254 and 365 nm). High-resolution mass spectra (HRMS) were obtained from a JEOL JMS-S3000 SpiralTOF (MALDI-TOF MS). Cyclic voltammetry (CV) measurements were performed by BAS ALS-600D electrochemical analyzer. Melting points were measured on a MPA100 Optimelt automated melting point system. Nuclear magnetic resonance (NMR) spectra were recorded on a JEOL JNM-ECA-600 (^{1}H 600 MHz, ^{13}C 150 MHz) or a JEOL ECA 600II spectrometer with Ultra COOL probe (^{1}H 600 MHz, ^{13}C 150 MHz). Chemical shifts for ^{1}H NMR are expressed in parts per million (ppm) relative to $CHCl_3$ (δ 7.26 ppm) or C_2DHCl_4 (δ 6.00 ppm). Chemical shifts for ^{13}C NMR are expressed in ppm relative to $CDCl_3$ (δ 77.16 ppm) or $C_2D_2Cl_4$ (δ 73.78 ppm). Data are reported as follows: chemical shift, multiplicity (s = singlet, d = doublet, t = triplet, m = multiplet, br = broad signal), coupling constant (Hz), and integration.

Synthesis of 1-Cl$_4$. Dichloromethane was purged by oxygen gas and dried by molecular sieves 4A overnight before use. To a solution of **2** (49.3 mg, 50.0 μmol, 1 equiv) in dichloromethane (10 mL) was added $MoCl_5$ (273 mg, 1.00 mmol, 20 equiv) at room temperature, and then the reaction mixture was stirred for 27 h under nitrogen atmosphere. The reaction was quenched by the addition of MeOH/$CHCl_3$ (1:1, 10 mL) solution, and the resultant solution was directly passed through a pad of silica gel with $CHCl_3$ eluent. The filtrate was evaporated in vacuo. The residue was dissolved in $CHCl_3$ and passed through a pad of silica gel again with *n*-hexane/$CHCl_3$ (1:1) eluent. The filtrate was evaporated in vacuo to afford **1-Cl$_4$** (20.1 mg, 36%) as a red solid: ^{1}H NMR (600 MHz, $CDCl_3$) δ 8.70 (d, J = 8.6 Hz, 2H), 8.68 (d, J = 8.5 Hz, 2H), 8.10 (d, J = 8.5 Hz, 2H), 8.06 (d, J = 8.5 Hz, 2H), 6.39 (s, 2H), 3.17−3.12 (m, 2H), 2.94−2.88 (m, 2H), 2.48 (dt, ^2J = 15.0, ^3J = 6.6 Hz, 2H), 2.35 (dt, ^2J = 15.1, ^3J = 7.0 Hz, 2H), 1.88−1.80 (m, 2H), 1.71−1.63 (m, 2H), 1.34−1.24 (m, 8H), 1.00−0.88 (m, 4H), 0.80 (t, J = 7.4 Hz, 6H), 0.74 (t, J = 7.4 Hz, 6H); ^{13}C NMR (150 MHz, $CDCl_3$) δ 146.9 (4°), 143.7 (4°), 138.1 (4°), 138.0 (4°), 132.5 (4°), 131.7 (4°), 130.1 (4°), 129.8 (4°), 129.4 (CH), 129.3 (CH), 129.1 (4°), 129.0 (4°), 128.0 (4°), 126.7 (4°), 126.6 (4°), 126.5 (4°), 125.3 (4°), 124.8 (4°), 124.3 (4°), 124.0 (4°), 123.4 (4°), 122.4 (CH), 121.0 (CH), 120.5 (CH), 119.7 (4°), 119.2 (4°), 34.6 (CH_2), 33.4 (CH_2), 30.4 (CH_2), 29.4 (CH_2), 22.7 (CH_2), 21.5 (CH_2), 13.9 (CH_3), 13.9 (CH_3); HRMS (MALDI-TOF MS) m/z calcd for $C_{66}H_{46}Cl_4S_4$ $[M]^+$ 1108.1207, found 1108.1209; mp >300 °C (recrystallized from chloroform).

Synthesis of 1. A mixture of **1-Cl$_4$** (4.9 mg, 4.4 μmol, 1 equiv), 5% Pd/C containing 55% water (18.9 mg, 4.00 μmol, 1 equiv), Et_3N (112 μL, 0.800 mmol, 180 equiv), and formic acid (30 μL, 0.80 mmol, 180 equiv) in pyridine (1 mL) was stirred at 130 °C for 72 h in a 20 mL Schlenk tube sealed with a J. Young O-ring tap. After the mixture was cooled to room temperature, the precipitate was dissolved in $CHCl_3$ (150 mL) and passed through a pad of silica gel with $CHCl_3$ eluent. The filtrate was evaporated in vacuo to afford **1** (4.0 mg, 94%) as a yellow solid: ^{1}H NMR (600 MHz, $C_2D_2Cl_4$) δ 8.95 (t, J = 8.3 Hz, 4H), 8.40 (d, J = 7.6 Hz, 2H), 8.37 (d, J = 7.7 Hz, 2H), 6.35 (s, 2H), 3.18−3.13 (m, 2H), 2.98−2.92 (m, 2H), 2.54 (dt, ^2J = 14.8, ^3J = 7.1 Hz, 2H), 2.45 (dt, ^2J = 15.1, ^3J = 7.2 Hz, 2H), 1.89−1.81 (m, 2H), 1.72−1.66 (m, 2H), 1.34 (septet, J = 7.4 Hz, 8H), 1.13−1.03 (m, 4H), 0.84−0.79 (m, 12H); ^{13}C NMR (150 MHz, $C_2D_2Cl_4$) δ 144.7 (4°), 140.7 (4°), 136.3 (4°), 135.5 (4°), 135.2 (4°), 134.1 (4°), 131.0 (4°), 130.9 (4°), 130.5 (4°), 129.0 (4°), 128.5 (4°), 128.2 (4°), 127.3 (CH), 127.2 (4°), 127.1 (CH), 124.2 (4°), 124.0 (4°), 123.6 (CH), 123.5 (4°), 122.5 (CH), 122.3 (4°), 122.2 (4°), 121.4 (CH), 120.5 (CH), 120.3 (CH), 120.0 (4°), 34.5 (CH_2), 33.3 (CH_2), 30.8 (CH_2), 29.7 (CH_2), 22.4 (CH_2), 21.3 (CH_2), 13.9 (CH_3), 13.8 (CH_3); HRMS (MALDI TOF-MS) m/z calcd for $C_{66}H_{50}S_4$ $[M]^+$ 970.2795, found 970.2779; mp >300 °C (recrystallized from nitrobenzene).

ASSOCIATED CONTENT

Supporting Information

The Supporting Information is available free of charge on the ACS Publications website at DOI: 10.1021/acs.joc.7b01540.

Details of computational study, photophysical measurements, and crystallographic data for **1-Cl$_4$** and **1** (PDF)

Crystallographic data for **1-Cl$_4$** and **1** (CIF)

Cartesian coordinates (XYZ)

AUTHOR INFORMATION

Corresponding Authors

*E-mail: ysegawa@nagoya-u.jp.

*E-mail: itami@chem.nagoya-u.ac.jp.

ORCID

Yasutomo Segawa: 0000-0001-6439-8546

Kenichiro Itami: 0000-0001-5227-7894

DOI: 10.1021/acs.joc.7b01540
J. Org. Chem. 2017, 82, 7745−7749

Notes

The authors declare no competing financial interest.

■ ACKNOWLEDGMENTS

This work was supported by the ERATO program from JST (JPMJER1302 to K.I.), the Funding Program for KAKENHI from MEXT (16K05771 to Y.S.), a grant-in-aid for Scientific Research on Innovative Areas "π-Figuration" (17H05149 to Y.S.), and the Noguchi Institute (to Y.S.). T.F. is a recipient of JSPS fellowship for young scientists. ITbM is supported by the World Premier International Research Center (WPI) Initiative, Japan. Calculations were performed using the resources of the Research Center for Computational Science, Okazaki, Japan.

■ REFERENCES

(1) Reviews on helicenes: (a) Shen, Y.; Chen, C.-F. *Chem. Rev.* **2012**, *112*, 1463. (b) Gingras, M. *Chem. Soc. Rev.* **2013**, *42*, 968. (c) Gingras, M.; Félix, G.; Peresutti, R. *Chem. Soc. Rev.* **2013**, *42*, 1007. (d) Gingras, M. *Chem. Soc. Rev.* **2013**, *42*, 1051.

(2) (a) Harvey, R. G. *Polycyclic Aromatic Hydrocarbons*; Wiley-VCH: New York, 1997. (b) Rieger, R.; Müllen, K. *J. Phys. Org. Chem.* **2010**, *23*, 315.

(3) (a) Mori, K.; Murase, T.; Fujita, M. *Angew. Chem., Int. Ed.* **2015**, *54*, 6847 and references cited therein. (b) Nejedlý, J.; Šámal, M.; Rybáček, J.; Tobrmanová, M.; Szydlo, F.; Coudret, C.; Neumeier, M.; Vacek, J.; Chocholoušová, J. V.; Buděšínský, M.; Šaman, D.; Bednárová, L.; Sieger, L.; Stará, I. G.; Starý, I. *Angew. Chem., Int. Ed.* **2017**, *56*, 5839.

(4) Benzohelicenes: (a) Klívar, J.; Jančařík, A.; Šaman, D.; Pohl, R.; Fiedler, P.; Bednárová, L.; Starý, I.; Stará, I. G. *Chem. - Eur. J.* **2016**, *22*, 14401. (b) Jančařík, A.; Rybáček, J.; Cocq, K.; Chocholoušová, J. V.; Vacek, J.; Pohl, R.; Bednárová, L.; Fiedler, P.; Císařová, I.; Stará, I. G.; Starý, I. *Angew. Chem., Int. Ed.* **2013**, *52*, 9970. (c) Laarhoven, W. H.; Nivard, R. J. F. *Tetrahedron* **1976**, *32*, 2445. (d) Laarhoven, W. H.; Cuppen, Th. J. H. M.; Nivard, R. J. F. *Tetrahedron* **1970**, *26*, 4865.

(5) Pyrenohelicenes: (a) Buchta, M.; Rybáček, J.; Jančařík, A.; Kudale, A. A.; Buděšínský, M.; Chocholoušová, J. V.; Vacek, J.; Bednárová, L.; Císařová, I.; Bodwell, G. J.; Starý, I.; Stará, I. G. *Chem. - Eur. J.* **2015**, *21*, 8910. (b) Bédard, A.-C.; Vlassova, A.; Hernandez-Perez, A. C.; Bessette, A.; Hanan, G. S.; Heuft, M. A.; Collins, S. K. *Chem. - Eur. J.* **2013**, *19*, 16295. (c) Hu, J.-Y.; Paudel, A.; Seto, N.; Feng, X.; Era, M.; Matsumoto, T.; Tanaka, J.; Elsegood, M. R. J.; Redshaw, C.; Yamato, T. *Org. Biomol. Chem.* **2013**, *11*, 2186. (d) Hu, J.-Y.; Feng, X.; Paudel, A.; Tomiyasu, H.; Rayhan, U.; Thuéry, P.; Elsegood, M. R. J.; Redshaw, C.; Yamato, T. *Eur. J. Org. Chem.* **2013**, *2013*, 5829. (e) Reference 4c.. (f) Hayward, R. J.; Hopkinson, A. C.; Leznoff, C. C. *Tetrahedron* **1972**, *28*, 439. (g) Vingiello, F. A.; Henson, P. D. *J. Org. Chem.* **1965**, *30*, 2842.

(6) Other laterally π-extended helicenes: (a) Fujikawa, T.; Preda, D. V.; Segawa, Y.; Itami, K.; Scott, L. T. *Org. Lett.* **2016**, *18*, 3992. (b) Rajeshkumar, V.; Stuparu, M. C. *Chem. Commun.* **2016**, *52*, 9957. (c) Schuster, N. J.; Paley, D. W.; Jockusch, S.; Ng, F.; Steigerwald, M. L.; Nuckolls, C. *Angew. Chem., Int. Ed.* **2016**, *55*, 13519. (d) Wang, X.-Y.; Wang, X.-C.; Narita, A.; Wagner, M.; Cao, X.-Y.; Feng, X.; Müllen, K. *J. Am. Chem. Soc.* **2016**, *138*, 12783. (e) Shiraishi, K.; Rajca, A.; Pink, M.; Rajca, S. *J. Am. Chem. Soc.* **2005**, *127*, 9312.

(7) (a) Wang, L.; Warburton, P. L.; Szekeres, Z.; Surjan, P.; Mezey, P. G. *J. Chem. Inf. Model.* **2005**, *45*, 850. (b) Treboux, G.; Lapstun, P.; Wu, Z.; Silverbrook, K. *Chem. Phys. Lett.* **1999**, *301*, 493. (c) Xu, F.; Yu, H.; Sadrzadeh, A.; Yakobson, B. I. *Nano Lett.* **2016**, *16*, 34.

(8) Fujikawa, T.; Mitoma, N.; Wakamiya, A.; Saeki, A.; Segawa, Y.; Itami, K. *Org. Biomol. Chem.* **2017**, *15*, 4697.

(9) $MoCl_5$-mediated cyclodehydrogenation: (a) Schubert, M.; Trosien, S.; Schulz, L.; Brandscheid, C.; Schollmeyer, D.; Waldvogel, S. R. *Eur. J. Org. Chem.* **2014**, *2014*, 7091. (b) Waldvogel, S. R.; Trosien, S. *Chem. Commun.* **2012**, *48*, 9109. (c) King, B. T.; Kroulík, J.; Robertson, C. R.; Rempala, P.; Hilton, C. L.; Korinek, J. D.; Gortari, L. M. *J. Org. Chem.* **2007**, *72*, 2279. (d) Kumar, S.; Manicham, M. *Chem. Commun.* **1997**, 1615. (e) Kovacic, P.; Lange, R. M. *J. Org. Chem.* **1963**, *28*, 968.

(10) Wynberg reported the conversion of pristine dithia[6]helicene to dithiahexa[7]circulene at 140 °C in a melt of $AlCl_3$/NaCl, see: Dopper, J. H.; Oudman, D.; Wynberg, H. *J. Org. Chem.* **1975**, *40*, 3398.

(11) (a) Rajca, A.; Miyasaka, M.; Xiao, S.; Boratyński, P. J.; Pink, M.; Rajca, S. *J. Org. Chem.* **2009**, *74*, 9105. (b) Severa, L.; Ončák, M.; Koval, D.; Pohl, R.; Šaman, D.; Císařová; Reyes-Gutiérrez, P. E.; Sázelová, P.; Kašička, V.; Teplý, F.; Slavíček, P. *Angew. Chem., Int. Ed.* **2012**, *51*, 11972.

(12) (a) Fujikawa, T.; Segawa, Y.; Itami, K. *J. Am. Chem. Soc.* **2015**, *137*, 7763. (b) Shan, L.; Liu, D.; Li, H.; Xu, X.; Shan, B.; Xu, J.-B.; Miao, Q. *Adv. Mater.* **2015**, *27*, 3418.

(13) Fujikawa, T.; Segawa, Y.; Itami, K. *J. Am. Chem. Soc.* **2016**, *138*, 3587.

(14) Martin, R. H.; Marchant, M. J. *Tetrahedron* **1974**, *30*, 347.

DOI: 10.1021/acs.joc.7b01540
J. Org. Chem. 2017, 82, 7745−7749